Local Symmetry of Hydrogen in Cubic and Tetragonal $SrTiO_3$ and $KTaO_3$:Li Determined by Polarized Raman Scattering

S. Klauer and M. Wöhlecke

Universität Osnabrück, Fachbereich Physik, Postfach 4469, D-4500 Osnabrück, Federal Republic of Germany

(Received 20 November 1991)

The OH stretch mode of hydrogen defect ensembles in cubic and tetragonal $SrTiO_3$ and $KTaO_3$:Li has been investigated with polarized Raman scattering. Introducing the Raman behavior type analysis to tetragonal crystals allows the determination of the local symmetry and proves for $SrTiO_3$ that protons vibrate along the O-O bonds on the edges of the oxygen octahedron. Moreover, the different local symmetries of OH dipoles in antiferrodistortive $SrTiO_3$ and $KTaO_3$:Li with polar off-center Li_K are reflected experimentally in the behavior type of the Raman scattering intensities.

PACS numbers: 63.20.Pw, 78.30.−j, 78.50.−w

Hydrogen centers in $SrTiO_3$ and $KTaO_3$:Li.— In most as-grown oxides the presence of hydrogen is revealed by a prominent, sharp ir absorption band at about 3500 cm^{-1} due to the OH stretching vibration. Elaborate polarized ir absorption studies have been performed with prototype perovskites, $SrTiO_3$ and $KTaO_3$:Li, including the application of external perturbations, such as uniaxial stress [1] and static electric fields [1–5], to lift the degeneracy among equivalent sites of the defect ensemble. Two contradicting atomistic models have been discussed by two groups [1,5]. Houde *et al.* [5] favor the cube face (CF) model, where the hydrogen vibrates on the faces between the O^{2-} and the Sr^{2+} (K^+) ion. In the competing octahedron edge (OE) model [1] the hydrogen vibrates along the O-O bonds of the oxygen octahedron. Both models are illustrated in Fig. 1 within the cubic unit cell.

In the cubic phase the protons are randomly distributed onto all the 24 energetically equivalent sites of the cube faces or all the O-O bonds, resulting in one single absorption line. Both $SrTiO_3$ and $K_{1-x}Li_xTaO_3$ undergo a cubic to tetragonal phase transition. In $SrTiO_3$ a zone-boundary phonon softens at $T_c \approx 105$ K, resulting in a unit cell doubling. A nonpolar antiferrodistortive phase results, where the oxygen octahedra in two neighboring cubes are pairwise counter-rotated around the tetragonal

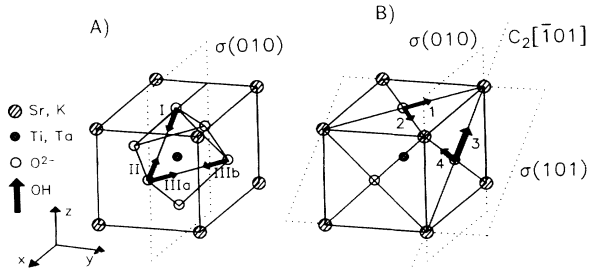

FIG. 1. Schematic representation of the two competing atomistic models for the incorporation of hydrogen in the perovskites $SrTiO_3$ and $KTaO_3$:Li: (a) the octahedron edge (OE) model; (b) the cube face (CF) diagonal model. The symmetry elements of the symmetry of the local environment present in the cubic phase are also indicated.

$z \| [001]$ axis. In $K_{1-x}Li_xTaO_3$ an order-disorder phase transition is believed to occur with a frozen-in off-center displacement of the Li_K ions along the cube axes, for $x \geq x_{crit} \approx 0.022$ [6]. The transition temperature T_c increases with the Li concentration [7].

The structural changes of the phase transition induce an energetic splitting of the OH band into three components $\nu_A < \nu_B < \nu_C$ for both systems. The central ir band ν_B is polarized perpendicular to the z axis and thus assigned to the subset of eight equivalent sites oriented in the x-y plane, i.e., sites 1 and 2 in the CF model and sites IIIa and IIIb in the OE model; see Fig. 1. The outer two bands ν_A and ν_C possess equal polarization components parallel and perpendicular to the z axis. This indicates an angle of 45° with respect to z. No assignments of ν_A and ν_C to sites 3 and 4 are given for the CF model [5]. The assignment of ν_A to the ensemble generated by site II and ν_C to ensemble I in the framework of the OE model [1] is not stringent. It is based only on plausible arguments drawn from the temperature dependence of the transition frequency and the splitting pattern in an external applied electric field.

Houde *et al.* [5] pointed out that in the OE model for the tetragonal phase of $SrTiO_3$ one has to consider two energetic inequivalent hydrogen positions, IIIa and IIIb, in the x-y plane, because due to the rotation of the octahedra one hydrogen approaches the two nearest corner Sr^{2+} ions, while the other one moves away. An accidental degeneracy for sites IIIa and IIIb has to be assumed in the OE model [1], while the CF model correctly predicts the observed threefold splitting. However, the CF model fails to explain the different electric field splitting of the bands ν_A and ν_C for an applied external field $\mathbf{E}_A \| [001]$. The related protons 3 and 4 are bound to equivalent oxygen ions in the CF model. Contrarily, in the OE model the related protons II and I are bound to inequivalent oxygen ions, thus easily justifying the assumption of different Lorentz factors necessary to account for the anisotropic field splitting behavior [1].

Both models have their drawbacks and can principally not be distinguished by polarized ir absorption spectroscopy because polarized light $\mathbf{E}_l$ interacts with the OH

defect with electric dipole moment $\mathbf{p}_{OH}$ according to $\mathbf{p}_{OH} \cdot \mathbf{E}_L$. Thus absorption experiments yield only information on the direction cosines of $\mathbf{p}_{OH}$. For each of the defect subsets I or II (IIIa or IIIb) according to the OE model there is a corresponding subset of dipoles 3 or 4 (1 or 2) in the CF model with the same orientation. Although both models are equivalent with respect to the *dipole directions,* they possess a different *local symmetry* of the environment of the vibrating OH molecule. We show how polarized Raman scattering data reflect these different symmetries and thus allow a clear decision between the two models exploited for $SrTiO_3$.

Outline of the behavior type method.—The behavior type method was introduced recently by Zhou, Goovaerts, and Shoemaker [8] for the analysis of polarized Raman scattering intensities of defect ensembles in *cubic* crystals. Our extension of the behavior type method to *tetragonal* crystals [9] will serve as the tool to obtain the maximum information on the local symmetry of the OH defect mode. The principle of the method is outlined below.

The symmetry point group O_1 determines the Raman tensor $\underline{\mathbf{T}} = (T_{ij})$ of a *single defect*, which connects the electric field polarization vectors $\mathbf{a}$ and $\mathbf{b}$ of the incident and scattered light, respectively. This information is partly obscured, because *polarized Raman intensities* $I_{\mathbf{a},\mathbf{b}}$ contain averages of the contributions $I_{\mathbf{a},\mathbf{b}}^{(n)}$ from all equivalent orientations in the *ensemble*, weighed by their population numbers $N^{(n)}$:

$$I_{\mathbf{a},\mathbf{b}} = \sum_{n=1}^{h} N^{(n)} I_{\mathbf{a},\mathbf{b}}^{(n)}, \tag{1}$$

where $I_{\mathbf{a},\mathbf{b}}^{(n)} \propto (\mathbf{a}\underline{\mathbf{T}}^{(n)}\mathbf{b})^2$. Rewriting Eq. (1) as

$$I_{\mathbf{a},\mathbf{b}} \propto \sum_{i,j,k,l=1}^{3} a_i b_j a_k b_l P_{ijkl}, \tag{2}$$

with

$$P_{ijkl} = \sum_{n=1}^{h} N^{(n)} T_{ij}^{(n)} T_{kl}^{(n)}$$

introduces the intensity parameters (IP) P_{ijkl}, which contain all the information on the $N^{(n)}$ and the Raman tensor. For later use, the shorthand notation of Ref. [8] shall be used to designate the most characteristic IP, namely, $q_i \propto P_{iiii}$, $r_i \propto P_{jjkk}$, and $s_i \propto P_{jkjk}$ for any $i \neq j \neq k$ from the set $\{1,2,3\}$.

Instead of solving Eqs. (2) for the $T_{i,j}$ the behavior type method focuses on the existence of simple algebraic relations between the IP of the ensemble induced by the symmetry of the single defect. The complete set of the 21 independent IP and the algebraic relations between them is called a *behavior type.* It was shown that even very simple relations, such as $x_i = 0$ or $x_i = \pm c x_j$ (for some integer or half-integer constant c and x_i denoting a specific IP), are very characteristic for specific symmetries O_1 of a mode, i.e., the related form of the Raman tensor. We want to emphasize that the measurable quantities $I_{\mathbf{a},\mathbf{b}}$ in general are linear combinations of the IP [Eq. (1)]. Very simple relations occur for $I_{x,x} \propto q_1$, $I_{y,y} \propto q_2$ as well as $I_{z,z} \propto q_3$, for $I_{y,z} \propto s_1$, $I_{x,z} \propto s_2$ as well as $I_{x,y} \propto s_3$, and for $I_{xy,xy} - I_{xy,x\bar{y}} \propto r_3 + s_3$. They prescribe the scattering geometries $(\mathbf{a},\mathbf{b})$ for the experiments described below.

Predictions of the extended behavior type method.—We have sketched in Fig. 1 the symmetry elements of the OH defect according to both models in the *cubic phase.* In the CF model a twofold axis $C_2[\bar{1}01]$ and two related vertical mirror planes $\sigma(010)$ and $\sigma(101)$ exist, while for the OE model there is only one mirror plane $\sigma(010)$. Unfortunately, the corresponding representative point groups [8] $O_1(\mathrm{CF}) = C_{2v}[110]$ for the CF and $O_1 = C_{1h}(010)$ for the OE model in the cubic systems result in the same cubic behavior type, preventing a distinction [10].

Therefore we extended the complete formalism of the behavior type method to *tetragonal systems* by compiling the set of tables necessary for a practical application [9]. The discriminative power of the method is strongly increased due to the less effective orientational average within the lower crystal symmetry. In particular, the behavior type for all representative modes with A-type transformation properties, to which the OH stretch mode belongs, remain different even for random distribution [9].

Because of the rotation of the octahedra in tetragonal $SrTiO_3$ only one symmetry element is preserved in the CF model, namely, $\sigma(010)$ for proton sites 3 and 4 and $\sigma(001)$ for sites 1 and 2. In the OE model the proton sites I and II are no longer situated in a mirror plane, while a $\sigma(001)$ mirror plane still exists for sites IIIa and IIIb. In Table I we have listed the tetragonal behavior type taken from Ref. [9] according to the site symmetries for the different models. The behavior type for the central band ν_B is the same for both models (line 3 of Table I), while the outer bands ν_A and ν_C behave differently with respect to IP s_3 (lines 1 and 2 of Table I). The related intensity $I_{x,y} \propto s_3$ is expected to be nonzero in the OE model $[O_1(\mathrm{OE}) = C_1]$ but must vanish because of the existence of the $\sigma(010)$ mirror plane in the CF model $[O_1(\mathrm{CF}) = C_{1h}(010)]$. The behavior of the IP s_i is thus a fingerprint of the local symmetry of the mode, in particu-

TABLE I. List of all possible local symmetries and resulting behavior types for OH defects in tetragonal $SrTiO_3$ and $KTaO_3$:Li, according to the different site symmetries O_1 in the OE and the CF model.

Local symmetry O_1	Main behavior type relations								
C_1	q_1	q_1	q_3	r_1	r_1	r_3	s_1	s_1	s_3
$C_{1h}(010)$	q_1	q_1	q_3	r_1	r_1	r_3	s_1	s_1	
$C_{1h}(001)$	q_1	q_1	q_3	r_1	r_1	r_3			s_3
$C_{1h}(110)$	q_1	q_1	q_3	r_1	r_1	q_1	s_1	s_1	s_3
$C_{2v}[110]$	q_1	q_1	q_3	r_1	r_1	q_1			s_3

lar the existence of vertical mirror planes.

Experiment and results.—The Raman spectra of the OH stretch mode in $SrTiO_3$ and $KTaO_3$:Li have been measured using a 6-W Ar ion laser beam (488 nm). A high degree of polarization, better than 100/1, and accurate alignment of polarizers and crystals to an accuracy of better than 1° were ensured using a novel method for precise crystal orientation [11].

Because polydomain samples would behave isotropically and hide the information coded in the IP, we prepared monodomain crystals. In $SrTiO_3$ this was achieved with uniaxial stress on (110) faces. We used unusual octagon shaped crystals with additional (100) and (001) faces to allow the measurement of all the IP s_i with one specimen. In $KTaO_3$:Li the tetragonal axis, and thus a monodomain state, was prescribed by an electric field $\mathbf{E}_{stat} \| [001]$, $E_{stat} \geq 3$ kV/cm. In both cases the achievement of the monodomain state was checked by the vanishing of the central ir absorption band ν_B for $\mathbf{E}_{stat} \| [001]$. We used the phase transition induced splitting of the OH band into three components [4] to determine the [Li] dependent T_c for the $KTaO_3$:Li sample to be 42 ± 2 K. The Raman spectra were taken at 24 K for $KTaO_3$:Li and 50 K for $SrTiO_3$, with a resolution of 1.5 and 2.0 cm^{-1}, respectively.

In the Raman spectra of OH in $SrTiO_3$ the three bands can clearly be resolved, see Fig. 2. It is important to notice that the IP $s_1 \propto I_{y,z}$ and $s_2 \propto I_{x,z}$ of the central band ν_B vanish for both $SrTiO_3$ and $KTaO_3$:Li, while the outer two bands ν_A and ν_C clearly show up. The IP $s_3 = I_{x,y}$ is actually different from zero for all three bands in $SrTiO_3$, but only for the central band ν_B in $KTaO_3$:Li, see Fig. 3.

Interpretation and discussion.—First we discuss the situation for $SrTiO_3$. We recall that in the framework of the OE model the horizontal x-y mirror plane $\sigma(001)$ containing the subset III dipoles is not affected by the rotation of the octahedra. Contrarily the vertical mirror symmetries of dipoles in subsets I and II are broken. Therefore we have $O_1(\mathrm{OE}) = C_{1h}(001)$ for the central band ν_B and simply $O_1 = C_1$ for the outer bands ν_A and ν_C. According to Table I the decision is based on the IP s_3 of the outer bands: It may be nonzero for the OE model, but is required to be zero in the CF model $[O_1(\mathrm{CF}) = C_{1h}(010)]$.

In Fig. 2 it is shown that the IP $s_1 \propto I_{y,z}$ and $s_2 \propto I_{x,z}$ are zero for the central band in accordance with the existence of the $\sigma(001)$ mirror plane predicted by both models. This also assures that the crystal was actually monodomain, and that the intensity $I_{x,y}$ corresponding to s_3 of ν_A and ν_C is not a remanent of the intense IP $q_1 = q_2 \propto I_{y,y}$ from polydomain regions of the crystal. Therefore we are sure that the nonzero IP s_3 for both outer bands, see the shadowed bands in Fig. 2, excludes a $\sigma(010)$ mirror plane, i.e., the validity of the CF model for $SrTiO_3$.

The situation for tetragonal $KTaO_3$:Li is different, because the reduction of the cubic symmetry is due to the off-center freezing-in of the Li_K ions. It is not *a priori* obvious whether the local symmetry of the hydrogen defect is remarkably influenced by the presence of the Li_K impurities. In the case of a negligible influence the vertical $\sigma(010)$ mirror plane is preserved for sites I and II in the OE model as well as for sites 3 and 4 of the CF model. This forces the IP s_3 for the outer bands to zero for both models on the stringent basis of symmetry considerations alone. On the other hand, an influence of Li_K would destroy that mirror plane in both models and a nonzero IP s_3 is expected.

The Raman spectra presented in Fig. 3 show that $s_3 \propto I_{x,y}$ is only detected for ν_B, whereas it vanishes for ν_A and ν_C indicating a negligible influence of the Li_K on the local mirror symmetry. The existence of a horizontal $\sigma(001)$ mirror plane in the OH dipole system related to ν_B (IIIa and IIIb in OE or 1 and 2 in CF) is suggested by the weak or even vanishing Raman intensity at frequency ν_B in the s_1 and s_2 spectra of Fig. 3.

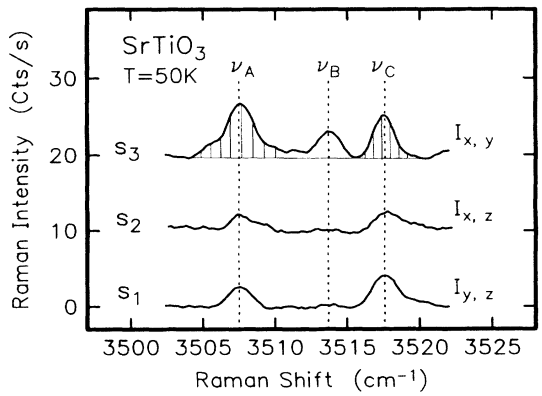

FIG. 2. Polarized Raman spectra of the OH stretch mode in monodomain tetragonal $SrTiO_3$, showing the behavior of the IP s_i ($i = 1,2,3$).

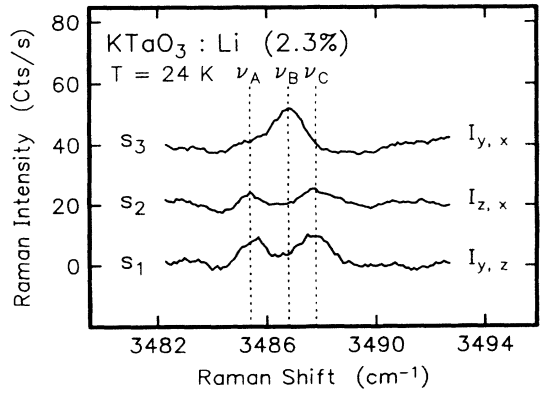

FIG. 3. Polarized Raman spectra of the OH stretch mode in monodomain tetragonal $KTaO_3$:Li, showing the behavior of the IP s_i ($i = 1,2,3$).

For $KTaO_3$:Li we have so far concluded that the local symmetry of the OH defect is not affected by the presence of the Li_K impurities. Unfortunately, the existence or nonexistence of mirror planes reflected in the behavior of the IP s_i does not allow a decision between the two models for $KTaO_3$:Li. In principle, a distinction is possible by an inspection of the behavior type of the central band ν_B. In addition to the observed horizontal $\sigma(001)$ mirror plane, a vertical $\sigma(110)$ mirror plane exists for the proton sites 1 and 2 in the CF model, which is not present for the sites IIIa and IIIb of the OE model. This difference is reflected in the IP r_3 for the central band ν_B. The IP r_3 must be equal to q_1 forced by the $\sigma(110)$ mirror plane present in the CF model (line 4 or 5 of Table I), but is independent when this specific symmetry element is absent, as is the case for the OE model (line 3 of Table I). However, the poor signal-to-noise ratio and, even more serious, the spectral overlap of the bands prevent a precise determination of the intensity of ν_B.

The negligible influence of Li_K impurities on the hydrogen site symmetry and the similar lattice structure favor the application of the OE model also for $KTaO_3$:Li. Consequently, this means that the difference between the polar off-center character of $KTaO_3$:Li and the antiferrodistortive structure of $SrTiO_3$ is reflected in the measured different behavior of the polarized Raman scattering intensities: The preserved vertical mirror plane in $KTaO_3$:Li forces the IP s_3 of the outer bands ν_A and ν_C to zero in contrast to $SrTiO_3$, where this symmetry is broken due to the rotation of the oxygen octahedra.

Financial support by the Deutsche Forschungsgemeinschaft (DFG), SFB 225/C1, is gratefully acknowledged.

[1] G. Weber, S. Kapphan, and M. Wöhlecke, Phys. Rev. B **34**, 8406 (1986).
[2] J. L. Brebner, S. Jandl, and Y. Lepine, Phys. Rev. B **23**, 3816 (1981).
[3] A. Jovanović, M. Wöhlecke, and S. Kapphan, J. Radiat. Eff. Defects Solids (to be published).
[4] A. Jovanović, Ph.D. thesis, University of Osnabrück, 1990 (unpublished).
[5] D. Houde, Y. Lépine, C. Pépin, S. Jandl, and J. L. Brebner, Phys. Rev. B **35**, 4948 (1987).
[6] H. Schremmer, W. Kleemann, and D. Rytz, Phys. Rev. Lett. **62**, 1896 (1989).
[7] J. J. van der Klink, D. Rytz, F. Borsa, and U. T. Höchli, Phys. Rev. B **27**, 89 (1983).
[8] J. F. Zhou, E. Goovaerts, and D. Schoemaker, Phys. Rev. B **29**, 5509 (1984).
[9] S. Klauer and M. Wöhlecke, Phys. Rev. B (to be published).
[10] S. Klauer and M. Wöhlecke, Ferroelectrics (to be published).
[11] S. Klauer and M. Wöhlecke (to be published).